An Experimental Study on Heat Transfer Characteristics Just Before Critical Heat Flux in Uniformly Heated Vertical Annulus Under a Wide Range of Pressures

Se-Young Chun, Sang-Ki Moon, Heung-June Chung, and Moon-Ki Chung

Korea Atomic Energy Research Institute

150 Dukjin-dong, Yuseung-gu, Daejeon 305-353, Korea

sychun@nanum.kaeri.kr

Masanori Aritomi

Research Laboratory for Nuclear Reactor, Tokyo Institute of Technology

2-12-1 Ohokayama, Meguro-ku, Tokyo, 152 Japan

Abstract

Water heat transfer experiments were carried out in a uniformly heated annulus with a wide range of pressure conditions. The local heat transfer coefficients for saturated water flow boiling have been measured just before the occurrence of the critical heat flux (CHF) along the length of the heated section. The trends of the measured heat transfer coefficients were quite different from the conventional understanding for the heat transfer of saturated flow boiling. This discrepancy was explained from the nucleate boiling in the liquid film of annular flow under high heat flux conditions. The well-known correlations were compared with the measured heat transfer coefficients. The Shah and Kandlikar correlations gave better prediction than the Chen correlation. However, the modified Chen correlation proposed in the present work showed the best agreement with the present data among correlations examined.

Key Words : heat transfer coefficient, saturated two-phase flow, critical heat flux, high pressure range, modified Chen correlation

1. Introduction

Accurate prediction of saturated flow boiling heat transfer coefficients is quite important in the design of boilers, evaporators, cooling systems of a nuclear power plant and other two-phase process equipment. A large number of correlations have been proposed for the boiling heat transfer coefficients. The flow boiling heat transfer phenomena appear to depend on the local two-phase flow patterns, fluid properties, heat transfer surface characteristics and geometric conditions. It is not easy to find out the boiling heat transfer coefficient correlation taking into account these

boiling flow situations, since the correlations are not always based theoretically, and an empirical approach is often necessary. Therefore, it is *important to have an understanding of the physical phenomena* and the mechanisms for adequate use of the correlations with reasonable accuracy.

In saturated two-phase flow boiling, the well-known correlations for heat transfer coefficient are *often expressed as the form incorporating both the* forced convective and the nucleate boiling terms. The flow pattern in the nucleate boiling region would be typically bubble and slug, and the forced convective boiling region is normally associated with annular flow. An early correlation, which is generally accepted, is that of Chen [1]. The correlation was given by a relatively simple additive form of two terms, that is, the contribution from the nucleate boiling based on Foster and Zuber's pool boiling correlation [2], and the forced convection contribution through the liquid film based on the single-phase Dittus-Boelter correlation [3]. Gungor and Winterton [4] developed a correlation based on the Chen form. A large database (3693 data points) including the annulus data was used in the development of the correlation. They employed Cooper's nucleate pool boiling correlation [5] for the nucleate boiling term. Bjorge et al. [6] developed a correlation in a superposition form of the heat flux for forced convection, nucleate boiling and incipient boiling. In the quality region greater than 0.05, they employed the slightly modified correlation of Traviss et al. [7] for the forced convection contribution, the Mikic and Rohsenow pool boiling correlation [8] for the nucleate boiling contribution, and the procedure of Bergles and Rohsenow [9] for the wall superheat at the incipient boiling point. Shah [10, 11] proposed a correlation using the boiling number B_0 and the convection number C_0. The Shah correlation is the most widely accepted one. A feature of the correlation is that the boiling number B_0 plays an important part and

the correlation does not include the viscosity term (i.e., the viscosity has no significant influence.). Recently, Kandlikar [12] developed a correlation that utilizes the boiling number, the convection number and the Froude number, which are the dimensionless parameters as used by Shah [11]. This correlation was based on about 5000 data points from tube experiments only.

The general consensus in the literature is that the Chen correlation is still widely used and is one of the most reliable correlations, in spite of much recent effort for the development of more accurate correlations. In the nuclear power industry, this correlation is adopted in modern thermal hydraulic design and system safety analysis codes [13-16]. However, the pressure conditions for the water data used in the development of the Chen correlation are ranges from 0.1 to 3.48 MPa, and the other correlations presented in the above references are mainly based on the heat transfer data in the pressures less than 7.5 MPa. The pressure dependence on these correlations has not been examined with more attention for a wide range of pressures until now.

This paper presents the results from the heat transfer experiments carried out in an internally heated annulus with a wide range of pressure conditions. In the present experiments, the local heat transfer coefficients for saturated water flow boiling have been measured along the length of the heated section just before the occurrence of the critical heat flux (CHF) at the top end of the uniformly heated section. In order to examine the pressure dependence on the well-known correlations, the heat transfer coefficients obtained in the present experiments are compared with those predicted by some important correlations. The Chen correlation is modified taking account of the behavior of the heat transfer just before CHF and the effect of pressure and quality on the heat transfer coefficient.
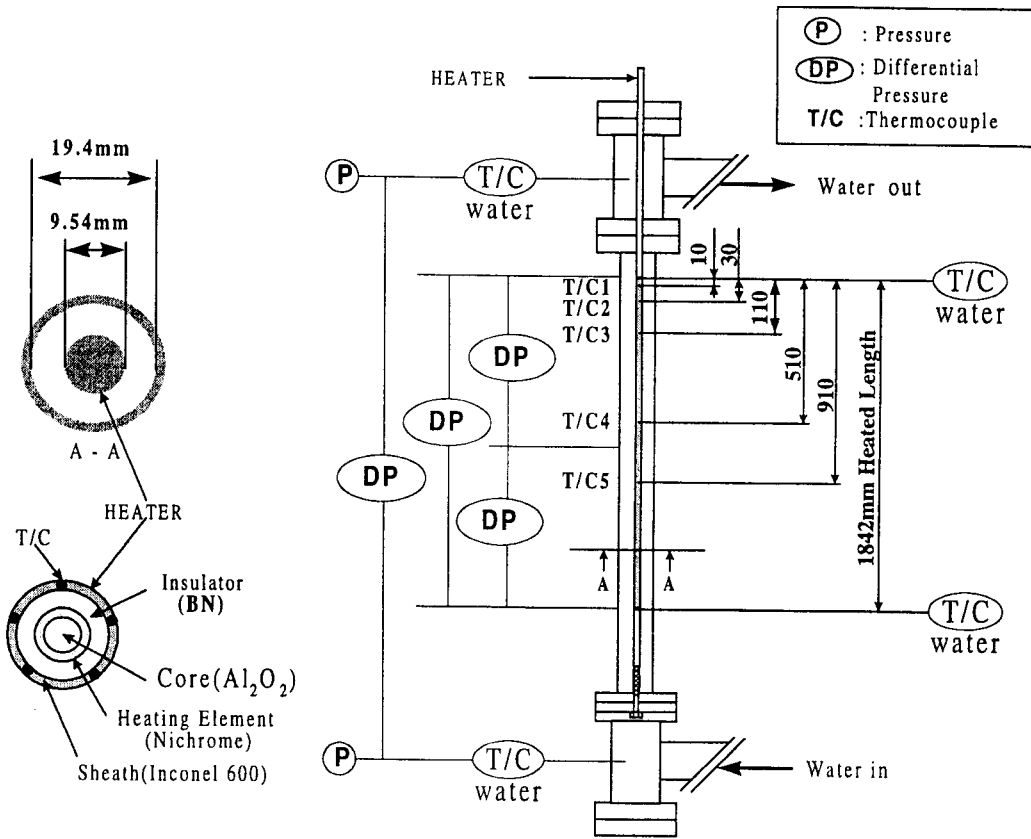
Fig. 1. Test Section Geometry and Thermocouple Locations

2. Experimental Description

2.1. Experimental Facility

The heat transfer experiments have been performed in the Reactor Coolant System thermal hydraulics loop (RCS loop) facility at the Korea Atomic Energy Research Institute (KAERI). A description of the experimental facility can be found in reference [17]. The test section used in this experimental work is described here in detail.

Figure 1 shows the details of the test section. The test section, which is an internally heated annulus flow channel, consists of an outer pipe with a 19.4 mm inside diameter and an inner heater rod with a 9.54 mm outer diameter having a heated length of 1842 mm at room temperature. The inner heater rod is heated indirectly by electricity with a uniform axial power distribution. The sheath and heating element of the heater rod are made of Inconel 600 and Nichrome, respectively. For measuring the heater rod surface temperatures, five Chromel-Alumel thermocouples with a sheath outer diameter of 0.5 mm are embedded on the outer surface of the heater rod. The temperature sensing points of these thermocouples are located at 10, 30, 110, 510 and 910 mm from the top end of the heated

section.

The main parameters measured in the present experiments are the water temperatures at the bottom and top of the heated section, the surface temperatures of the heater rod, the pressures at the inlet and outlet plenums, the differential pressures in the test section, the flow rate of the test section inlet and the power applied to the heater rod. All the electrical signals from the sensors and transmitters are processed and analyzed by a data acquisition system (DAS) consisting of A/D (analog to digital) converters and a workstation computer. The uncertainties of the measuring system were estimated from the calibration of sensors and the accuracy of the equipment, according to a propagation error analysis based on the Taylor's series method [18]. The evaluated maximum uncertainties of pressure, flow rate and heater surface temperature were less than ± 0.3 %, ± 1.5 % and ± 0.7 K of the readings in the range of interest, respectively. The uncertainty of the heat flux calculated from the applied power was always less than ± 1.8 % of the readings. Before starting a set of experiments, pretests (i.e., heat balance tests) were carried out to estimate the heat loss in the test section, so the heat loss in the test section was included in the value of the actual heat flux.

2.2. Experimental Procedure and Conditions

The experiments have been performed by the following procedure. First, the flow rate, inlet subcooling and system pressure are established at desired levels, and the power is applied to the heater rod of the test section and increased gradually in small steps while the test section inlet conditions are kept at constant values. The period between the power steps are chosen to be sufficiently long so that the loop can be stabilized at a steady state condition. This process continues until the CHF occurs at the top of the heated section. The occurrence of CHF can be identified by a sharp increase in the heater rod surface temperature. Whenever the CHF is detected, the heater power is automatically reduced or tripped to prevent any damage to the heater rod. At a power level just before the CHF condition, the five heater rod surface temperatures along the length of the heated section and the other experimental parameters are automatically measured and gathered at the same time by the DAS. As the loop approaches the CHF conditions, oscillations of the heater rod surface temperatures are frequently observed at the top end of the heated section (T/C 1 and 2 in Fig. 1). This oscillation indicates that the dryout or breakup of the liquid flow on the surface of the heater rod intermittently occurs. The situation that the heater surface is not wetted by water is out of scope of the present work. In order to obtain the heat transfer coefficient while the surface is sufficiently cooled by water flow, for the locations of T/C 1 and 2, the averages of the 100 data points of the minimum temperature values in the oscillation are used in the analysis.

In the present work, 814 heat transfer coefficient data points for saturated flow boiling were obtained. The experimental conditions under which the present data have been collected are as follows:

- pressure   0.57 ~ 15.01 MPa
- mass flux   200 ~ 650 kg/m^{2}s
- inlet subcooling   85 ~ 353 kJ/kg
- thermodynamic
  equilibrium quality   0 ~ 0.536
- heat flux   520 ~ 1765 kW/m^2

The conditions in the test section were controlled within the deviations of ± 1.9 % for the pressure, ± 2.3 % for the mass flux and ± 6.2 % for the inlet subcooling from the above values. The pressures are the local values at the locations of

each thermocouple on the heater rod surface, calculated from the pressures at the inlet and outlet plenums on the assumption that the pressures along the test section linearly vary between the inlet and outlet plenums. The inlet subcooling is determined from the water temperature at the bottom end of the heated section and the pressure at the inlet plenum. Thermodynamic equilibrium qualities are the local values at the locations of each thermocouple on the heater rod surface calculated from the heat balance in the heated section.

3. Experimental Results and Discussions

Accurate modeling and a trustworthy evaluation of the two-phase flow boiling heat transfer require a good understanding of the local two-phase flow pattern, since the heat transfer mechanisms are closely related to the local two-phase flow regimes. Therefore, the two-phase flow pattern under the present experimental conditions is examined using the flow regime transition criteria in the vertical tubes of Mishima and Ishii [19], which can be applied over wide ranges of parameters as well as to high-pressure steam-water flow. In the annuli, the two-phase flow situations may be different from those of the tubes because of the existence of the effects of the annular gap and cold wall. For instance, in the case of annuli, unlike the flow in vertical tube, the largest concentration of the bubbles would not occur in the middle of the annular gap. However, the application of Mishima and Ishii's transition criteria to the present condition is useful to understand the general two-phase flow behavior. The two-phase flow regime transition is usually expressed by the relation between the superficial liquid and vapor velocities. The locations of the flow pattern transitions along the heated section can be calculated from a relationship between the superficial vapor velocity
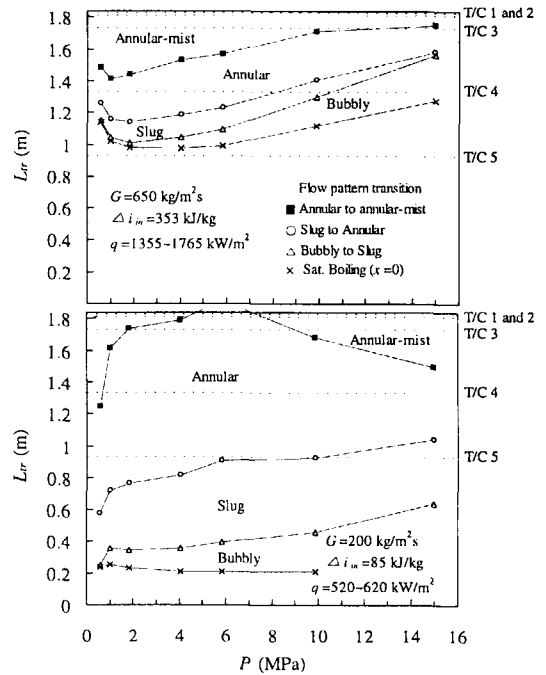
Fig. 2. Locations of Two-phase Flow Pattern Transitions Along the Length of the Heated Section

j_g and the quality x_{tr} at flow pattern transitions. The location L_{tr} of the transition is calculated by the following equation

$$x_{tr} = \rho_g j_g / G,\qquad(1)$$

and

$$L_{tr} = \frac{A_f G(x_{tr} i_{lg} + \Delta i_{in})}{\pi d q},\qquad(2)$$

where ρ_g, G, A_f, i_{lg}, Δi_{in}, d and q are the vapor density, the mass flux, the cross sectional flow area, the latent heat of vaporization, the inlet subcooling enthalpy of the heated section, the diameter of heater rod and the heat flux, respectively. The flow regime transition locations along the heated section are shown as a function of pressure in Fig. 2. The superficial vapor
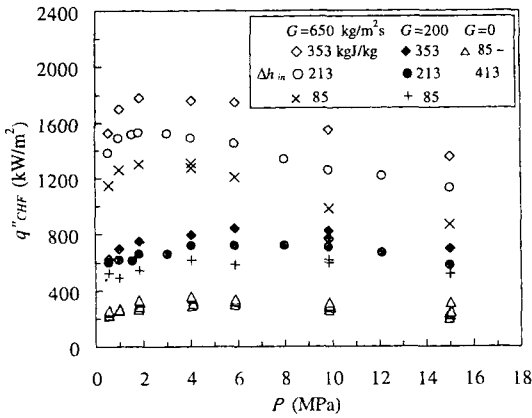
Fig. 3. Effect of Pressure on CHF (from Chun et al. [17])

Fig. 4. Measured Heat Transfer Coefficients as a Function of Pressure

velocity j_g was calculated using the hydraulic equivalent diameter D_{hy} ($=4 \times$ flow area/wetted perimeter) in the flow regime transition criteria of Mishima and Ishii [19]. This figure shows that the two-phase flow pattern at the top end of the heated section (the locations of T/C 1 and 2, see Fig. 1) is the annular-mist flow in the present experimental conditions. On the other hand, in the middle part of the heated section (the location of T/C 5), the bubbly and slug flow patterns including a partially annular flow become dominant. The single-phase flow data in which the quality is negative are not used in this work. Chun et al. [17] conducted the CHF experiments using the same test section as the present experiments and observed such variation of the CHF with pressure as shown Fig. 3. Therefore, it should be noted that Fig. 2 does not give a general trend about the mutual relation between the two-phase flow pattern and pressure, because the heat flux is restricted by the power level of the heater rod just before the occurrence of CHF in the present experiments.

The heat transfer coefficient for two-phase flow boiling $h_{TP,exp}$ is calculated by the following equation
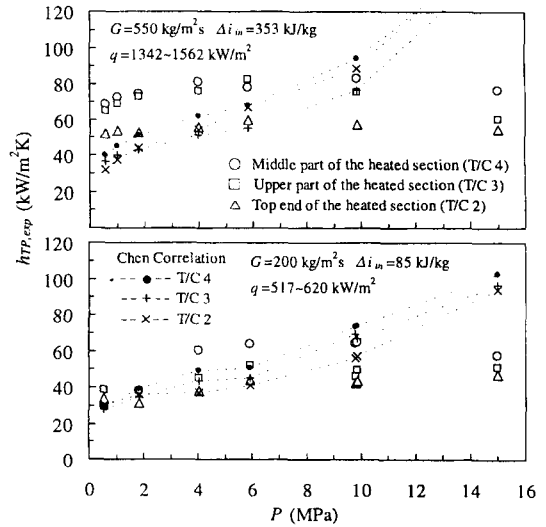
$$h_{TP,exp} = \frac{q}{(T_w - T_{sat})}, \qquad (3)$$

where T_{sat} is the saturation temperature of water, which is determined from the pressure at the location of the thermocouple for measuring the heater rod surface temperature T_w. Typical variations of the local heat transfer coefficients with pressure are shown in Fig. 4. Some results from the calculation by the Chen correlation given in this figure are discussed in later Chapters. The heat transfer coefficients at a given pressure were obtained at the same heat flux, since the surface temperatures along the heated section were measured at the same time, while the heat flux conditions vary with pressure. The heat transfer coefficients slowly increase up to a pressure of 6 MPa, as the pressure increases. In the high-pressure region beyond 10 MPa, the heat transfer coefficients are nearly constant or give indications of the slight decrease with increasing pressure. The behavior of the heat transfer coefficients in Fig. 4 appears to come under the influence of the variation of the CHF with pressure such as shown
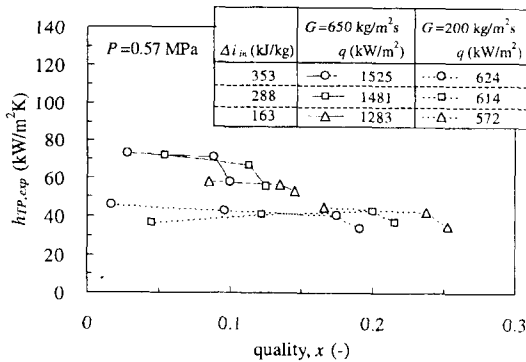
Fig. 5(a). Measured Heat Transfer Coefficients as a Function of Quality at P=0.57 MPa
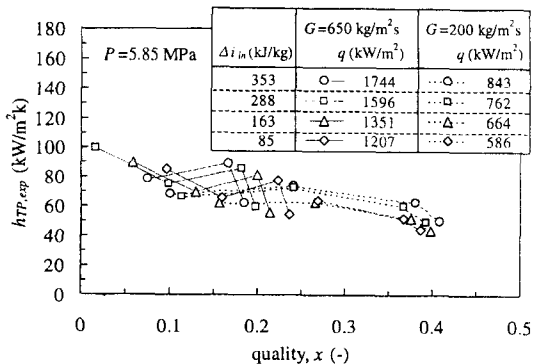

Fig. 5(b). Measured Heat Transfer Coefficients as a Function of Quality at P=5.85 MPa
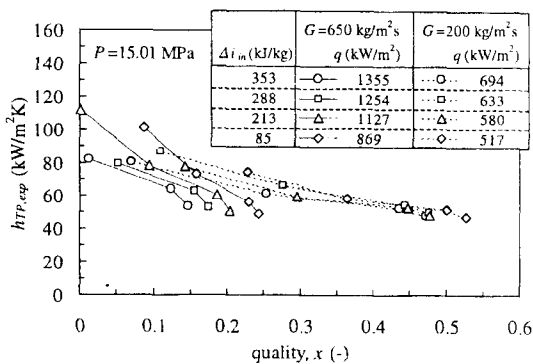

Fig. 5(c). Measured Heat Transfer Coefficients as a Function of Quality at P=15.01 MPa

in Fig. 3, since the heat transfer coefficient generally increases with increasing heat flux. In addition, Figure 4 shows that the heat transfer coefficients at the top end of the heated section are always less than those at the middle part.

The variation of the heat transfer coefficients along the heated length, in the conventional understand, is characterized as follows [20, 21]. The heat transfer coefficient is nearly constant or gradually increases with quality in the low quality region where the nucleate boiling mechanism is dominant, and in the downstream high quality region, where the forced convective boiling mechanism comes dominant, increases with quality and is nearly independent of heat flux. The increasing heat transfer coefficient with quality is obstructed by the occurrence of CHF. The heat transfer coefficients as a function of quality are shown in Fig. 5. The quality along the heated length with a uniform heat flux distribution varies linearly. Each data point in this figure corresponds to the locations of T/C 2, 3, 4 and 5, in order from the data point with the highest quality. The heat transfer coefficients at the top end (T/C 2) of the heated section are sharply reduced from the values in the upper part (T/C 3). This corresponds with a trend of the heat transfer coefficients at the top end of the heated section in Fig. 4. The two-phase flow pattern at the top end of the heated section is judged to be the annular flow from Fig. 2. The sharp reduction of the heat transfer coefficient is most likely to be associated with the liquid film flow situation on the heated surface with an imminent local dryout just before the CHF occurrence.

As shown in Fig. 5, the behavior of the heat transfer coefficients with quality depends upon the pressure. In Fig. 5(a), the heat transfer coefficients at upper and middle parts (T/C 3, 4 and 5) of the heated section keep a nearly constant value. At medium pressure of 5.85 MPa(Fig. 5(b)), the heat

transfer coefficients show a temporary reduction (T/C 4) followed by an increase (T/C 3) with quality for the mass flux of 650 kg/m²s, and a constant at middle part (T/C 5 and 4) followed by a slight decrease at the upper part (T/C 3) for the mass flux of 200 kg/m²s. Figure 5(c) shows the decreasing trend of the heat transfer coefficients with quality at high pressure of 15.01 MPa over the entire quality rang. The trends of the heat transfer coefficients in Fig. 5 are quite different from the conventional understanding of saturated flow boiling heat transfer. In practice, some cases, which show the behavior similar to the trends of the heat transfer coefficients in Fig. 5(b) and 5(c). have been reported [12, 22]. The conventional understanding mentioned above applies to the case of the low heat flux equipment, such as evaporators and steam boilers. In such cases, no bubble nucleation occurs at heating surface in the liquid film of annular flow where the forced convective boiling mechanism is dominant, because of the suppression of nucleate boiling. Therefore, heat is transferred by evaporation on the liquid film surface. Most of the heat transfer coefficients in the present experiments were obtained under annular or annular-mist flow conditions. However, it appears that the nucleate boiling occurs in the liquid film because a very high heat flux is supplied to the heater surface. The heat transfer mechanism, in this case, is most likely to be associated with the nucleate boiling, in spite of the fact that the flow pattern is mostly annular flow. It seems that this leads to the complicated trend of the heat transfer coefficients with quality in Fig. 5.

When the ratio of the two-phase heat transfer coefficient h_{TP} to the single-phase liquid heat transfer coefficient h_l based on the total (or liquid component) is plotted against the reciprocal of the Martinelli parameter X_{tt}, the heat transfer coefficient in the forced convective boiling region,
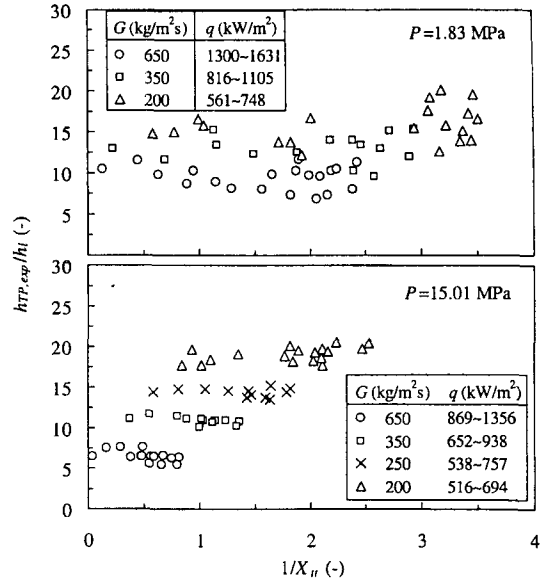

Fig. 6. Variations of Heat Transfer Coefficient Ratio with Reciprocal of the Martinelli Parameter

in general, is correlated in the following form

$$\frac{h_{TP}}{h_l} = A\left(\frac{1}{X_{tt}}\right)^n,\qquad(4)$$

where A and n are the constants, which have the positive values. The Martinelli parameter is given by the following expression [20]

$$X_{tt} = \left(\frac{1-x}{x}\right)^{0.9}\left(\frac{\rho_g}{\rho_l}\right)^{0.5}\left(\frac{\mu_l}{\mu_g}\right)^{0.1},\qquad(5)$$

where x, ρ and μ are the quality, the density and the dynamic viscosity, respectively. The subscript g and l denote the vapor and liquid phases, respectively. The heat transfer coefficient ratio $h_{TP,exp}/h_l$ is shown as a function of $1/X_{tt}$ in Fig. 6. The coefficient h_l is calculated from the Dittus-Boelter correlation using the Reynolds number of the liquid phase Re_l (=$G(1-x)D/\mu_l$). For the calculation of the Reynolds number, a hydraulic equivalent diameter D_{hy} is used in place of the tube

Table 1. Heat Transfer Correlations for Saturated Two-phase Flow Boiling (1 of 2)

Reference	Correlation

Chen [1]
 	
Mainly based on tube data
 	
For water data,
$0.1 < P < 3.5$ MPa
$0.06 < v < 4.48$ m/s
$6.3 < q < 2400$
     kW/m^2
$0.01 < x < 0.71$
 	
Estimates for F and S are given by reference [14].
	$h_{TP} = h_{FC} + h_{NB}$
	
	$h_{FC} = 0.023 \dfrac{k_l}{D} (\mathrm{Re}_l)^{0.8} (\mathrm{Pr}_l)^{0.4} F$
	
	$h_{NB} = 0.00122 \left(\dfrac{k_l^{0.79} c_{pl}^{0.45} \rho_l^{0.49}}{\sigma^{0.5} \mu_l^{0.29} i_{lg}^{0.24} \rho_g^{0.24}} \right) \Delta T_{sat}^{0.24} \Delta P_{sat}^{0.75} S$
	
	$F = 1.0$ for $X_{tt}^{-1} \le 0.1$, $F = 2.35\left(X_{tt}^{-1} + 0.213\right)^{0.736}$ for $X_{tt}^{-1} > 0.1$
	
	and $S = \left[1 + 0.12\,\mathrm{Re}_{TP}\right]^{-1.14}$ for $\mathrm{Re}_{TP} < 32.5$
	
	       $S = \left[1 + 0.42\left(\mathrm{Re}_{TP}\right)^{0.78}\right]^{-1}$ for $32.5 \le \mathrm{Re}_{TP} < 70$
	       $S = 0.0797$ for $\mathrm{Re}_{TP} \ge 70$
	
	where $\mathrm{Re}_{TP} = \min\left(70, \mathrm{Re}_l\, F^{1.25} \times 10^{-4}\right)$

Shah [11]
 	
Mainly based on tube data
 	
For water data,
$6.17 < D_{hy} < 25.4$
     mm
$0.1 < P < 17.4$ MPa
$67.8 < G < 1383.4$
     kg/m^{2}s
$44 < q < 789$ kW/m^2
$0 < x < 0.70$
	For vertical tube
	
	$h_{FC} = 0.023 \dfrac{k_l}{D} (\mathrm{Re}_l)^{0.8} (\mathrm{Pr}_l)^{0.4} \left(\dfrac{1.8}{C_o^{0.8}} \right)$
	
	If $C_o > 0.1$, $h_{NB} = 0.023 \dfrac{k_l}{D} (\mathrm{Re}_l)^{0.8} (\mathrm{Pr}_l)^{0.4} \left(\dfrac{230 B_o^{0.5}}{0.0003} \right)$ for $B_o > 230 B_o^{0.5}$
	
	$h_{NB} = 0.023 \dfrac{k_l}{D} (\mathrm{Re}_l)^{0.8} (\mathrm{Pr}_l)^{0.4} \left(\dfrac{1 + 46 B_o^{0.5}}{0.0003} \right)$ for $B_o < 1 + 46 B_o^{0.5}$
	
	If $1.0 > C_o > 0.1$, $h_{NB} = 0.023 \dfrac{k_l}{D} (\mathrm{Re}_l)^{0.8} (\mathrm{Pr}_l)^{0.4} F B_o^{0.5} exp(2.74 C_o^{-0.1})$
	
	If $C_o < 0.1$, $h_{NB} = 0.023 \dfrac{k_l}{D} (\mathrm{Re}_l)^{0.8} (\mathrm{Pr}_l)^{0.4} F B_o^{0.5} exp(2.74 C_o^{-0.15})$
	
	where $F = 14.7$ for $B_o > 0.0011$ and $F = 15.43$ for $B_o < 0.0011$
	The higher of the two heat transfer coefficients, h_{FC} and h_{NB}, gives the two-phase heat transfer coefficient h_{TP}.

Gungor and Winterton [4]
 	
Based on tube and annuli data
 	
For water data,
$2.95 < D_{hy} < 25.4$ mm
$0.1 < P < 19.8$ MPa
$59.2 < G < 8179.3$
     kg/m^{2}s
$4.7 < q < 2280$
     kW/m^2
$0 < x < 0.70$
	For vertical upward flow in saturated boiling
	$h_{TP} = h_{FC} + h_{NB}$
	
	$h_{FC} = 0.023 \dfrac{k_l}{D} (\mathrm{Re}_l)^{0.8} (\mathrm{Pr}_l)^{0.4} E$
	
	$h_{NB} = 55 P_r^{0.12} (-log_{10} P_r)^{-0.55} M^{-0.5} q^{0.67} S$
	
	where $E = 1 + 24000 B_o^{1.16} + 1.37\left(X_{tt}^{-1}\right)^{0.86}$
	
	      $S = \left(1 + 1.15 \times 10^{-6} E^2 \mathrm{Re}_l^{1.17}\right)^{-1}$

Table 1. Heat Transfer Correlations for Saturated Two-Phase Flow Boiling (2 of 2)

Reference	Correlation
Bjorge et al. [6] Based on tube data Water data only $2.95<D<25.4$ mm $0.0624<P<7.43$ MPa $54.2<G<3930$ kg/m²s $22<q<4570$ kW/m² $0.01<x<0.65$	For the high quality region $(x > 0.05)$ $$q = q_{FC} + q_{NB}\left[1 - \left(\frac{\Delta T_{sat,ib}}{\Delta T_{sat}}\right)^3\right]$$ $$q_{FC} = \frac{\text{Re}_l^{0.9} \text{Pr}_l F(X_{tt}) k_l}{F_2 D} \Delta T_{sat}$$ where $F(X_{tt}) = 0.15[X_{tt}^{-1} + 2.0(X_{tt}^{-1})^{0.32}]$ $F_2 = 5\text{Pr}_l + 5ln(1 + 5\text{Pr}_l) + 2.5ln(0.0031\text{Re}_l^{0.812})$ for $\text{Re}_l > 1125$ $F_2 = 5\text{Pr}_l + 5ln[1 + \text{Pr}_l(0.0964\text{Re}_l^{0.585} - 1)]$ for $50 < \text{Re}_l < 1125$ $F_2 = 0.0707\text{Pr}_l \text{Re}_l^{0.5}$ for $\text{Re}_l < 50$ $$\frac{q_{NB}}{\mu_l i_{lg}}\left(\frac{g_o \sigma}{g(\rho_l - \rho_g)}\right)^{0.5}$$ $$= 1.89 \times 10^{-14} \frac{k_l^{0.5} \rho_l^{2.125} c_{pl}^{2.375} \rho_g^{0.125}}{\mu_l i_{lg}^{0.875}(\rho_l - \rho_g)^{1.125} \sigma^{0.625} T_{sat}^{0.125}} \Delta T_{sat}^3$$ where $\Delta T_{sat,ib} = \frac{8\sigma T_{sat} h_{FC}}{k_l i_{lg}(\rho_l - \rho_g)}$
Kandlikar [12] Based on tube data For water data, $5<D<32$ mm $0.11<P<6.42$ MPa $67<G<8179$ kg/m²s $4.7<q<2280$ kW/m² $0<x<0.70$	For vertical upward flow in saturated water boiling $$h_{TP} = 0.023\frac{k_l}{D}(\text{Re}_l)^{0.8}(\text{Pr}_l)^{0.4}\left(C_1 C_o^{C_2} + C_3 B_o^{C_4}\right)$$ where for the convective region $C_1 = 1.1360$, $C_2 = -0.9$, $C_3 = 667.2$, $C_4 = 0.7$ for the nucleate boiling region $C_1 = 0.6683$, $C_2 = -0.2$, $C_3 = 1058.0$, $C_4 = 0.7$ The heat transfer coefficient at any given condition is evaluated using the two sets of constants for the two regions, and the higher of the two heat transfer coefficient values represents the two-phase heat transfer coefficient value.

inner diameter D. At pressure of 1.83 MPa, the ratio $h_{TP,exp}/h_l$ gives indications of the slight decrease for small values of $1/X_{tt}$ (i.e., small values of quality) and the increase for larger values of $1/X_{tt}$ (i.e., larger values of quality). The figure for the pressure of 15.01 MPa gives a typical result in the present experiments. The ratio $h_{TP,exp}/h_l$ is kept at constant over the entire range of $1/X_{tt}$ and there is no increasing trend of $h_{TP,exp}/h_l$ for larger values of $1/X_{tt}$. In all pressure conditions, excepting the pressure of 1.83 MPa, the ratio

$h_{TP,exp}/h_l$ is a constant or slightly increases with $1/Xtt$ without the increase in the large value range of $1/X_{tt}$. In addition, the ratio $h_{TP,exp}/h_l$ is strongly influenced by the mass flux rather than the heat flux. In the region where the forced convective boiling mechanism is dominant, the ratio $h_{TP,exp}/h_l$ is expected to increase with $1/X_{tt}$ from the form of Eq. (4). Figure 6, therefore, shows that the dominant heat transfer mechanism in this experimental condition appears to be mostly nucleate boiling and this, moreover, is consistent

Table 2. Comparison of Correlations with Experimental Data

Correlation	Equivalent diameter	Mean error (%)	Absolute mean error (%)	RMS error (%)
Chen [1]	D_{hy}	1.3	22.4	29.1
	D_{he}	-32.6	33.9	37.2
Shah [11]	D_{hy}	-6.7	19.2	23.4
	D_{he}	-25.3	27.2	31.0
Gungor and	D_{hy}	24.4	27.5	37.7
Winterton [4]	D_{he}	74.4	74.4	70.4
Bjorge et al. [6]	D_{hy}	-41.0	41.0	43.3
	D_{he}	-44.1	44.1	46.1
Kandlikar [12]	D_{hy}	3.0	19.9	26.6
	D_{he}	-17.5	23.8	27.4
Present work	D_{hy}	1.1	10.4	13.1
Eq. (10)	D_{he}	-	-	-

$$\text{mean error} = \frac{1}{N}\sum_{N=1}^{N}\left(\frac{h_{TP,pred}-h_{TP,exp}}{h_{TP,exp}}\right)\times100, \quad \text{absolute mean error} = = \frac{1}{N}\sum_{N=1}^{N}\left|\frac{h_{TP,pred}-h_{TP,exp}}{h_{TP,exp}}\right|\times100$$

$$\text{RMS error} = \sqrt{\frac{1}{N}\sum_{N=1}^{N}\left(\frac{h_{TP,pred}-h_{TP,exp}}{h_{TP,exp}}\right)^2}\times100$$

with the above discussion for Fig. 5.

4. Comparison with Existing Correlations

The Chen [1], Shah [11], Gungor and Winterton [4], Bjorge et al., [6] and Kandlikar [12] correlations for saturated two-phase flow boiling have been selected for a comparison with the present data. In the comparison with the Bjorge et al. correlation, a set of equations for the high quality region of their correlation was used. The correlation forms and parameter ranges are presented in Table 1. These correlations are mainly based on the heat transfer data in the tubes. A characteristic of heat transfer depends upon the two-phase flow situation, and

consequently, the heat transfer coefficient in annuli may be different from that of tubes. For the prediction of heat transfer coefficients in annulus geometry, an equivalent diameter is applied to the correlations. The correlations are compared with the present experimental data by using both the hydraulic equivalent diameter D_{hy} and the heated equivalent diameter D_{he} (4 × flow area/heated perimeter) as the equivalent diameter. The results of the comparison of the correlations with all of the present data are listed in Table 2.

The Chen, Shah and Kandlikar correlations using the heated equivalent diameter always underpredict the present data and result in larger errors than those using the hydraulic equivalent diameter. For the flow boiling heat transfer of
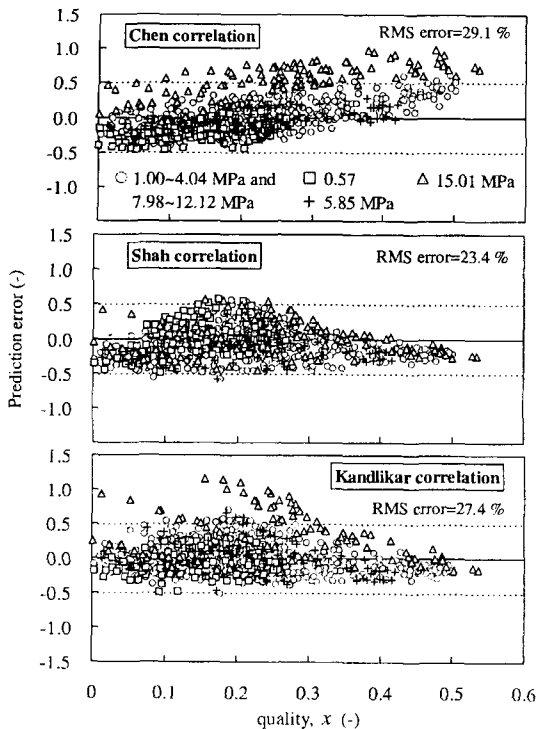
Fig. 7. Comparison of Measured Heat Transfer Coefficients with the Existing Correlations, where Prediction Error= $(h_{TP,pred} - h_{TP,exp})/h_{TP,exp}$

water in vertical annuli, Shah [11] and Gungor and Winterton [4] found out that the use of the hydraulic equivalent diameter for annular gaps greater than 4 mm, and the heated equivalent diameter for gaps less than 4 mm gives successful predictions. This finding is demonstrated in the present comparison of the correlation with the present data. Therefore, the hydraulic equivalent diameter is used for the correlations examined in the present work, since the annular gap of the test section in the present experiments is 4.93 mm.

The Gungor and Winterton correlation considerably overpredicts and the Bjorge et al. correlation underpredicts the present data. These two correlations give poor agreement for both equivalent diameters. The Gungor and Winterton correlation was developed with the aid of the

database including the annulus data. However, the examination done by Gungor and Winterton showed that the predictive ability for annuli of their correlation is considerably inferior to that for tube [4].

In order to illustrate the prediction performance of each correlation, the prediction errors are plotted as a function of quality with pressure as a parameter in Fig. 7. The Chen correlation tends to underpredict the present data in the low quality region and to overpredict in the high quality region, for the pressures less than 12 MPa. The prediction for the pressure of 15.01 MPa shows much higher values than the experimental data. As can be seen from Fig. 7, the prediction performance of the Chen and Kandlikar correlations comes under the influence of pressure. The comparison of the measured heat transfer coefficients with the Chen correlation in Fig. 4 indicates that the prediction error moves simply from underprediction to overprediction as the pressure increases because the heat transfer coefficients calculated by the correlation monotonously increase with increasing pressure. The Kandlikar correlation gives very good agreement (absolute mean error of 17.4 %) without quality dependence for the entire pressure range except 15.01 MPa, but considerably overpredicts some data at a pressure of 15.01 MPa in the low and medium quality regions. It seems to result from the fact that the pressure range of the heat transfer database used in the development of the correlation is from 0.11 to 6.42 MPa. The Shah correlation shows good agreement with all of the present data without remarkable pressure and quality dependencies.

5. Modification of the Chen Correlation

As can be seen from Table 2 and Fig. 7, the predictive capability of the Chen correlation [1] is
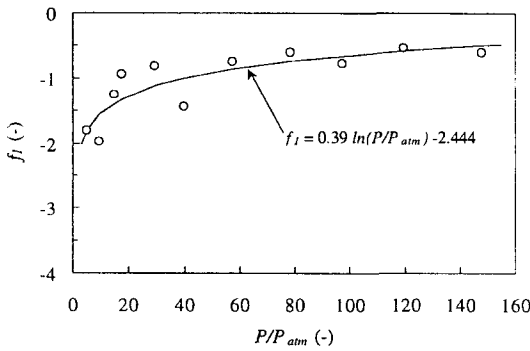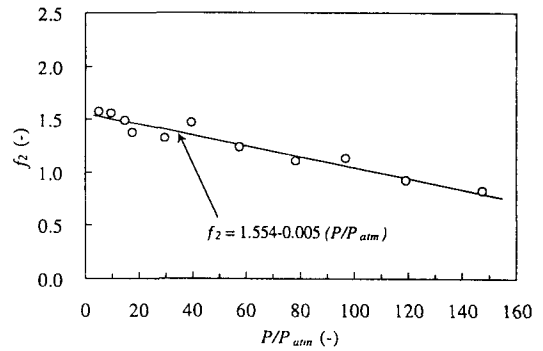
Fig. 8. Variation of f_1 with Pressure

Fig. 9. Variation of f_2 with Pressure

not so good, compared to the Shah and Kandlikar correlations, for the present data. This is due to the insufficient reflection of dependence of the heat transfer coefficient on a wide range of the quality or pressure.

In order to modify the Chen correlation, the correction factor f_c, which is a function of quality x and pressure P, is introduced as follows:

$$f_c = \frac{h_{TP,exp}}{h_{TP,Chen}}, \qquad (6)$$

where $h_{TP,exp}$ is the measured value of the heat transfer coefficient obtained from the present experiments and $h_{TP,Chen}$ is the heat transfer coefficient value predicted by the Chen correlation using the equivalent hydraulic diameter. The predicted heat transfer coefficient $h_{TP,Chen}$ by the Chen correlation monotonously increases with increasing pressure as shown Fig. 4. It appears that the prediction error of the Chen correlation in Fig. 7 slightly increases with quality x for a given pressure. Therefore, it is assumed that f_c decreases linearly with increasing x for a given pressure. The equation form of f_c can be expressed as follows:

$$f_c = \{f_1(P)\}x + f_2(P), \qquad (7)$$

where f_1 and f_2 are a function of pressure.

For each pressure, the values of fc calculated by Eq. (6) are plotted as a function of quality x, and the values of f_1 and f_2 are then estimated at each pressure. The equation forms of f_1 and f_2 are determined by plotting the values of f_1 and f_2 as a function of pressure. Figures 8 and 9 show the values of f_1 and f_2 with pressure. These equation forms are expressed as

$$f_1 = 0.39 \times ln\left(\frac{P}{P_{atm}}\right) - 2.444, \qquad (8)$$

and

$$f_2 = 1.554 - 0.005 \times \left(\frac{P}{P_{atm}}\right), \qquad (9)$$

where P_{atm} is the standard atmospheric pressure. The modified Chen correlation $h_{TP,pred}$ is

$$h_{TP,pred} = h_{TP,Chen}\left\{\left[0.39 \times ln\left(\frac{P}{P_{atm}}\right) - 2.444\right]x - 0.005 \times \left(\frac{P}{P_{atm}}\right) + 1.554\right\} \quad (10)$$

Figures 10 and 11 show the comparison of the heat transfer coefficient values predicted by Eq. (10) with the present data. It can be seen from these figures that Eq. (10) gives very good agreement with all of the present data. As can be seen from Table 2, the prediction using Eq. (10) yields the lowest RMS error (13.1 %) among the
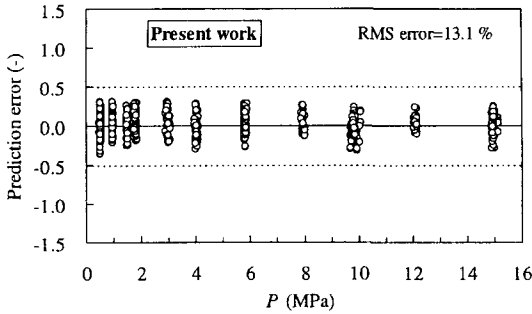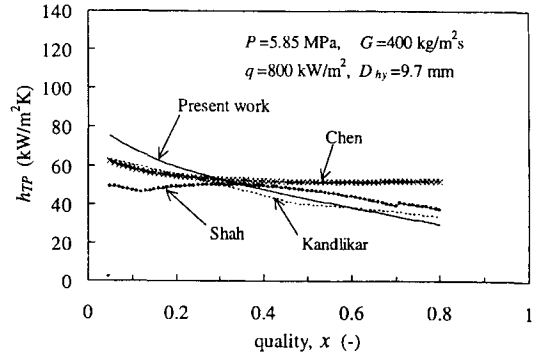
Fig. 10. Comparison of the Measured Heat Transfer Coefficients with the Modified Chen Correlation-Pressure Dependence
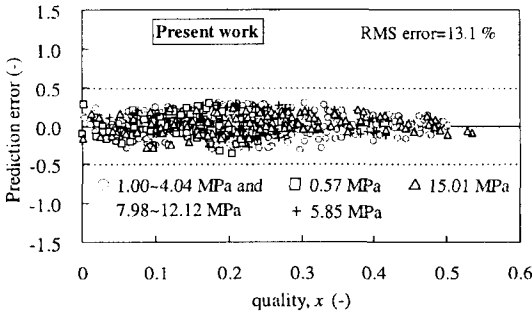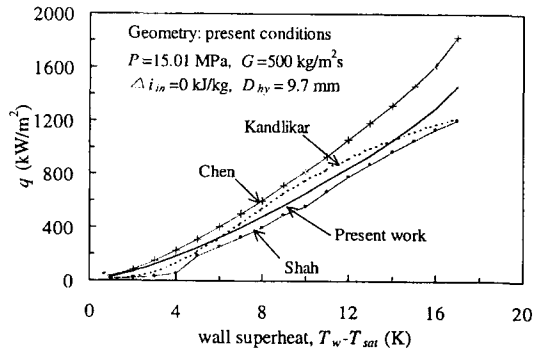

Fig. 11. Comparison of the Measured Heat Transfer Coefficients with the Modified Chen Correlation-Quality Dependence

Fig. 12. Comparison of the Modified Chen Correlation with the Existing Correlations-Two-phase Heat Transfer Coefficient as a Function of Quality

Fig. 13. Comparison of the Modified Chen Correlation with the Existing Correlations-Heat Flux as a Function of Wall Superheat

correlations examined.

The comparison between Eq. (10) and the Chen, Shah and Kandlikar correlations are shown in Figs. 12 and 13. The calculation of the heat transfer coefficients with the Chen correlation requires an iteration scheme, since the Chen correlation needs a wall superheat ΔT_{sat} in the calculation of the nucleate boiling term h_{NB} and does not include the heat flux term. In Fig. 13, the wall superheats ΔT_{sat} are the values at the top end of the heated section in the present test section, assuming the inlet subcooling $\Delta i_{in}=0$. Figures 12 and 13 show that the modified Chen correlation proposed in the present work is consistent with the parametric

trends of the Shah and Kandlikar correlations. It is observed that for the present geometry conditions, the heat transfer coefficient calculated by the Chen, Shah and Kandlikar correlations have the increasing trend with quality in the low heat flux region less than 300 kW/m². This implies that the forced convective boiling in the heat transfer mechanism becomes dominant as the heat flux decreases. The correction factor f_c is based on the heat transfer coefficient data, which were obtained

under very high heat flux conditions just before the CHF and are expected to be the nucleate boiling dominated region. Therefore, the proposed modified Chen correlation is applicable to the high heat flux conditions where the nucleate boiling mechanism is dominant.

6. Conclusions

The local heat transfer coefficients for saturated flow boiling have been measured along the length of the heated section under the high heat flux conditions just before the CHF occurrence. The behavior of the heat transfer coefficients measured in the present experiments is quite different from the conventional understanding for the heat transfer of saturated flow boiling. This can be explained from the consideration that the *dominant heat transfer mechanism in the present* experimental conditions is the nucleate boiling in the liquid film of the annular flow.

The results of the comparison of the existing correlations with the present data show that the Shah and Kandlikar correlations give reasonable predictions. The Chen correlation shows poor prediction, compared to the Shah and Kandlikar correlations. In the present comparison, the use of the hydraulic equivalent diameter gives better prediction, compared to the use of the heated equivalent diameter. This observation is consistent with the finding of shah, and Gungor and Winterton.

The Chen correlation is modified using the present data to reflect the dependence of the heat transfer coefficient on pressure and quality. This modified correlation gives the best predictions among the correlations examined in the present work.

Acknowledgment

Nomenclature

A	constant in Eq. (4)
A_f	cross sectional flow area, m^2
B_o	boiling number, $q/(Gi_{lg})$
C_o	convection number, $[(1-x)/x]^{0.8}(\rho_g/\rho_l)^{0.5}$
c_p	specific heat, J/kgK
D	inner diameter of tube, m
D_{he}	heated equivalent diameter, m
D_{hy}	hydraulic equivalent diameter, m
d	diameter of heater rod, m
f_c	correction factor for the Chen correlation
f_1 and f_2	expressed by Eqs. (8) and (9)
G	mass flux, kg/m^{2}s
g	gravitational acceleration, m/s^2
g_o	constant, 1 kgm/Ns^2
h	heat transfer coefficient, W/m^{2}K
Δh_{in}	inlet subcooling enthalpy of the heated section in Fig. 3, J/kg
i_{lg}	latent heat of vaporization, J/kg
Δi_{in}	inlet subcooling enthalpy of the heated section, J/kg
j	superficial velocity, m/s
k	thermal conductivity, W/mK
L	distance from the bottom end of the heated section, m
M	molecular weight
N	number of data points
n	constant in Eq. (4)
P	pressure, MPa
ΔP_{sat}	difference between the saturation pressure corresponding to the wall temperature and the local pressure, Pa
P_r	Prandtl number, $\mu c_p/k$
q	heat flux, W/m^2
$q"CHF$	critical heat flux in Fig. 3, kW/m^2
Re_l	Reynolds number of the liquid phase, $G(1-x)D/\mu_l$

T	temperature, K
ΔT_{sat}	wall superheat, T_w-T_{sat}, K
v	water velocity, m/s
X_{tt}	Martinelli parameter, $[(1\text{-}x)/x]^{0.9}(\rho_g/\rho_l)^{0.5}$ $(\mu_l/\mu_g)^{0.1}$
x	thermodynamic equilibrium quality
μ	dynamic viscosity, Ns/m^2
ρ	density, kg/m^3
σ	surface tension, N/m

Subscripts

atm	standard atmosphere
Chen	Chen's correlation
exp	experiment
FC	forced convection
g	vapor phase
ib	value at the incipient boiling point
l	liquid phase
NB	nucleate boiling
p_{red}	predicted
r	reduced
sat	saturation
TP	two-phase
tr	location of the two-phase flow pattern transition
w	heated wall

References

1. J. C. Chen, "A correlation for boiling heat transfer to saturated fluids in convective flow," *Industrial and Engineering Chemistry, Process Design and Development*, Vol. 5, No. 3, 322-329 (1966).

2. H. K. Forster and N. Zuber, "Dynamics of vapour bubbles and boiling heat transfer," *Journal of AIChE*, Vol. 1(4), 531-535 (1955).

3. F. W. Dittus and L. M. K. Boelter, "Heat transfer in automobile radiators of the tubular," *Publications in Engineering, University of California*, Vol. 2, 443-461 (1930).

4. K. E. Gungor and R. H. S. Winterton, "A general correlation for flow boiling in tubes and annuli," *Int. J. Heat Mass Transfer*, Vol. 29, 351-358 (1986).

5. M. G. Cooper, "Saturation nucleate pool boiling. A simple correlation," *1st U. K. National Conference on Heat Transfer*, Vol. 2, 785-793 (Industrial and Chemical Engineering Symposium Series No. 86, 1984).

6. R. W. Bjorge, G. R. Hall and W. M. Rohsenow, "Correlation of forced convection boiling heat transfer data," *Int. J. Heat Mass Transfer*, Vol. 25, 753-757 (1982).

7. D. P Traviss, W. M. Rohsenow and A. B. Baron, "Forced convection condensation inside tube: A heat transfer equation for design," *ASHRAE Reprint* No. 2272 RP-63 (1972).

8. B. B. Mikic and W. M. Rohsenow, "A new correlation of pool boiling data including the effect of heating surface characteristics," ASME, *J. Heat Transfer*, Vol. 91, 245 (1969).

9. A. E. Bergles and W. M. Rohsenow, "The determination of forced convection, surface boiling heat transfer," ASME, *J. Heat Transfer*, Vol. 86, 365-372 (1964).

10. M. M. Shah, "A new correlation for heat transfer during boiling flow through pipes," *ASHRAE Trans.*, Vol. 82, Part 1, 66-86 (1976).

11. M. M. Shah, "Chart correlation for saturated boiling heat transfer: equations and further study," *ASHRAE Trans.*, Vol. 88, Part 2, 185-196 (1982).

12. S. G. Kandlikar, "A general correlation for saturated two-phase flow boiling heat transfer inside horizontal and vertical tubes," *ASME, J. Heat Transfer*, Vol. 112, 219-228 (1990).

13. D. R. Liles, J. H. Mahaffy et al., "TRAC-PF1, An advanced best-estimate computer program for pressurized water reactor analysis, draft,"

Los Alamos National Laboratory (1984).

14. "RELAP5 code manual, NUREG/CR-5535," Idaho National Engineering and Environment Lab., USNRC (1995).

15. M. J. Thurgood, J. M. Kelly, T. E. Guidotti, R. J. Kohrt and K. R. Croweel, "COBRA/TRAC, A thermal-hydraulic code for transient analysis of nuclear reactor vessel and primary coolant system, equation and constitutive models," NUREG/CR-3046, PNL-4385, Vol. 1, R4 (1983).

16. L. K. H. Leung, K. F. Rudzinski, B. Verma, D. C. Groeneveld and A. Vasic, "Thermalhydraulics evaluation package (TEP V3.0), A user-friendly software package for evaluating thermalhydraulics parameters in tube and bundles," *Proc. 9th Int. Topl. Mtg. Nucl. Reactor Thermal-Hydraulics*, San Francisco, USA, Advanced Code Development, session B.4 (1999).

17. S. Y. Chun H. J. Chung, S. K. Moon, S. K. Yang, M. K. Chung and M. Aritomi, "Effect of pressure on critical heat flux in uniformly heated vertical annulus under low flow conditions," *Nuclear Engineering and Design*, Vol. 203, 159-174 (2001).

18. "ANSI/ASME PTC 19.1, ASME performance test codes, supplement on instruments and apparatus, part 1, measurement uncertainty," (1985).

19. M. Mishima and M. Ishii, "Flow regime transition criteria for upward two-phase flow in vertical tube," *Int. J. Heat Mass Transfer*, Vol. 27, 723-737 (1984).

20. J. G. Collier and J. R. Thome, "Convective boiling and condensation, 3rd edition," Oxford University Press, 249-256 (1994).

21. Y. Aounallah, D. B. R. Kenning, P. B. Whalley and G. F. Hewitt, "Boiling heat transfer in annular flow," *Proc. 7th Int. Heat Transfer Conference*, Munchen, Germany, Vol. 4, 193-199 (1982).

22. T. Kandlbinder, V. V. Wadekar and G. F. Hewitt, "Mixture effects for flow boiling of a binary hydrocarbon mixture," *Proc. 11th Int. Heat Transfer Conference*, Kyongju, Korea, Vol. 2, 303-308 (1998).